Preconditioned residual methods for solving steady fluid flows

Jean-Paul Chehab, Marcos Raydan

Preconditioned residual methods for solving steady fluid flows

Jean-Paul Chehab* Marcos Raydan†

Abstract

We develop free-derivative preconditioned residual methods for solving nonlinear steady fluid flows. The new scheme is based on a variable implicit preconditioning technique associated to the globalized spectral residual method. It is adapted for computing in a numerical way the steady state of the bi-dimensional and incompressible Navier-Stokes equations (NSE). We use finite differences for the discretization and consider both the primary variables and the stream function-vorticity formulations of the problem. Our numerical results agree with the ones in the literature and show the robustness of our method for Reynolds numbers up to $Re = 5000$.

1 Introduction

The art of preconditioning has become a widely used approach to accelerate numerical methods for solving linear as well as non-linear problems. For linear systems, the technique is already widely developed and very well understood. However, the art of preconditioning nonlinear iterative methods remains a challenge, and it is not so well understood.

The emergence of non-monotone residual methods as the one introduced by Barzilai and Borwein in optimization [1, 11, 24], and its globalized versions which enhances its robustness [19, 20, 21, 25], gives the possibility of solving efficiently large scale nonlinear problems, incorporating in a natural way a preconditioning strategy. Non-monotone globalization strategies for nonlinear problems have become popular in the last few years. These strategies make it possible to define globally convergent algorithms without monotone decrease requirements. The main idea behind non-monotone strategies is that, frequently, the first choice of a trial point, along the search direction hides significant information about the problem structure and that such knowledge can be destroyed by the decrease imposition.

In this work we adapt and extend, for the steady fluid flow problem, the ideas introduced in [19, 20]. In particular, we add a preconditioning strategy fully described in [9]. The so-called *lid driven cavity* problem, which corresponds to the computation of the evolutive (or the steady) flow of the bi-dimensional incompressible Navier-Stokes equations (NSE) on a rectangular cavity, displays classical benchmarks for testing nonlinear solvers, because of the amount of numerical solutions refereed, and also of the numerical difficulty of the problem. To compute steady states, two approaches are commonly considered: on one hand, the time-dependent methods which consist in computing the steady state as the equilibrium solution of the evolutive NSE (for Reynolds numbers that are lower than that of the bifurcation value) by time marching scheme and, on the other hand, the steady methods which consist in solving the steady NSE by fixed point or Newton-like schemes. It is a well-known fact that the solution of the steady NSE is more difficult since it requires very robust schemes, especially as the Reynolds number Re increases. The literature on that topic is very rich from, e.g., the relaxation schemes proposed by Crouzeix [10] to the more recent defect-correction methods, see e.g. [30] and the references therein. However these methods are very closely related to the structure of the NSE and use a linearization of the equation at each step.

*Laboratoire de Mathématiques Paul Painlevé, (CNRS) UMR 8524, Université de Lille, France, **chehab@math.univ-lille1.fr** and Laboratoire de Mathématiques, CNRS, UMR 8628, Equipe ANEDP, Université Paris Sud, Orsay, France

†Departamento de Computacíon, Facultad de Ciencias, Universidad Central de Venezuela, Ap. 47002, Caracas 1041-A, Venezuela **mraydan@kuaimare.ciens.ucv.ve**

Our aim in this article is to compute the solution of the steady NSE by a preconditioned version of the spectral residual method, with globalization. The method we introduce here is general and uses only the solution of the linear part of the equation that can be obtained efficiently with a fast solver (e.g., FFT, multigrid).

The article is organized as follows: first, in section 2, after recalling the definition of the globalization strategy for the spectral gradient scheme, we derive our new algorithm combining the dynamical and the optimization approaches. Then, in Section 3, we adapt the discretization of the steady bi-dimensional incompressible Navier-Stokes equations to the framework of the nonlinear scheme. Finally, in section 4, as a numerical illustration, we present the solution of steady NSE for different Reynolds numbers (up to $Re = 5000$). We solve the problem in primary variable as well as in stream function-vorticity formulation. Our results agree with the ones in the literature and show the robustness of the proposed method.

2 The basic algorithm

In a general framework, let us consider the nonlinear system of equations

$$F(x) = 0, \tag{1}$$

where $F : \Re^n \to \Re^n$ is a continuously differentiable mapping. This framework generalizes the nonlinear systems that appear after discretizing the steady state models for fluid flows, to be discussed later in this work.

For solving (1), some new iterative schemes have recently been presented that use in a systematic way the residual vectors as search directions [19, 20]. i. e., the iterations are defined as

$$x_{k+1} = x_k \pm \lambda_k F(x_k), \tag{2}$$

where $\lambda_k > 0$ is the step-length and the search direction is either $F(x_k)$ or $-F(x_k)$ depending on which one is a descent direction for the merit function

$$f(x) = \|F(x)\|_2^2 = F(x)^T F(x). \tag{3}$$

These ideas become effective, and competitive with Newton-Krylov ([2, 3, 18]) schemes for large-scale nonlinear systems, when the step lengths are chosen in a suitable way. The convergence of (2) is attained when it is associated with a free-derivative non-monotone line search, fully described in [20], and that will be discussed in the forthcoming subsections.

For the choice of the step-length $\lambda_k > 0$, there are many options for which convergence is guaranteed. We propose to use the non-monotone spectral choice that has interesting properties, and is defined as the absolute value of

$$\lambda_k = \frac{s_{k-1}^T s_{k-1}}{s_{k-1}^T y_{k-1}}, \tag{4}$$

where $s_{k-1} = x_k - x_{k-1}$, and $y_{k-1} = F(x_k) - F(x_{k-1})$. Obtaining the step length using (4) requires a reduced amount of computational work, accelerates the convergence of the process, and involves the last two iterations in such a way that incorporates first order information into the search direction [1, 11, 24, 15].

2.1 The preconditioned version

In order to present the preconditioned version of (2) we extend the ideas discussed in [21], for unconstrained minimization, to the solution of (1).

The well-known and somehow ideal Newton's method for solving (1), from an initial guess x_0, can be written as

$$x_{k+1} = x_k - J_k^{-1} F(x_k), \tag{5}$$

where $J_k = J(x_k)$, and $J(x)$ is the Jacobian of f evaluated at x.

Recently [21] a preconditioned scheme, associated to the gradient direction, was proposed to solve unconstrained minimization problems. For solving (1) the iterates associated with the preconditioned version of (2) are given by

$$x_{k+1} = x_k + \lambda_k d_k, \tag{6}$$

where $d_k = \pm C_k\, F(x_k)$, C_k is a nonsingular approximation to J_k^{-1}, and the scalar λ_k is given by

$$\lambda_k = (\lambda_{k-1})\frac{d_{k-1}^T F(x_{k-1})}{d_{k-1}^T y_{k-1}}. \tag{7}$$

In (6), if $C_k = I$ (the identity matrix) for all k, then $d_k = \pm F(x_k)$, λ_k coincides with (4), and so the method reduces to (2). On the other hand, if the sequence of iterates converges to x^*, and we improve the quality of the preconditioner such that $C(x_k)$ converges to $J^{-1}(x^*)$ then, as discussed in [9], λ_k tends to 1 and we recover Newton's method, which possesses fast local convergence under standard assumptions [12]. In that sense, the iterative scheme (6) is flexible and allows intermediate options, by choosing suitable approximations C_k, between the identity matrix and the inverse of the Jacobian matrix. For building suitable approximations to $J^{-1}(x_k)F(x_k)$ we will test implicit preconditioning schemes that do not require the explicit computation of C_k, and that will be described in Section 2.3.

2.2 Globalization strategy

In order to guarantee convergence of the preconditioned residual algorithm previously described, from any initial guess, we need to add a globalization strategy. This is certainly an interesting feature, specially when dealing with highly nonlinear flow problems and high Reynolds numbers. To avoid the derivatives of the merit function, which are not available, we will adapt the recently developed strategy of La Cruz et al [20] to our preconditioned version.

Assume that $\{\eta_k\}$ is a sequence such that $\eta_k > 0$ for all $k \in \mathbb{N}$ and

$$\sum_{k=0}^{\infty} \eta_k = \eta < \infty. \tag{8}$$

Assume that $0 < \gamma < 1$ and $0 < \sigma_{min} < \sigma_{max} < \infty$. Let M be a positive integer. Let τ_{min}, τ_{max} be such that $0 < \tau_{min} < \tau_{max} < 1$.

Given $x_0 \in \mathbb{R}^n$ an arbitrary initial point, the algorithm that allows us to obtain x_{k+1} starting from x_k is given below.

Global Preconditioned Residual (GPR) Algorithm.

Step 1.

- Choose σ_k such that $|\sigma_k| \in [\sigma_{min}, \sigma_{max}]$ (e.g., the spectral coefficient)
- Build C_k (an inverse preconditioner)
- Compute $\bar{f}_k = \max\{f(x_k), \ldots, f(x_{\max\{0,k-M+1\}})\}$.
- Set $d \leftarrow -\sigma_k C_k\, F(x_k)$.
- Set $\alpha_+ \leftarrow 1$, $\alpha_- \leftarrow 1$.

Step 2.

If $f(x_k + \alpha_+ d) \leq \bar{f}_k + \eta_k - \gamma\alpha_+^2 \|d\|_2^2$ then

Define $d_k = d, \alpha_k = \alpha_+, x_{k+1} = x_k + \alpha_k d_k$

else if $f(x_k - \alpha_- d) \leq \bar{f}_k + \eta_k - \gamma\alpha_-^2 \|d\|_2^2$ then
Define $d_k = -d, \alpha_k = \alpha_-, x_{k+1} = x_k + \alpha_k d_k$
else
choose $\alpha_{+new} \in [\tau_{min}\alpha_+, \tau_{max}\alpha_+]$, $\alpha_{-new} \in [\tau_{min}\alpha_-, \tau_{max}\alpha_-]$,
replace $\alpha_+ \leftarrow \alpha_{+new}$, $\alpha_- \leftarrow \alpha_{-new}$
and go to Step 2.

Remark 1. As we will see later, the coefficient σ_k will be intended to be an approximation of the quotient $\|F(x_k)\|^2/\langle J(x_k)F(x_k), F(x_k)\rangle$. This quotient may be positive or negative (or even null).
Remark 2. As discussed in [20], the algorithm is well defined, i. e., the backtracking process (choosing α_{+new} and α_{-new}) is guaranteed to terminate successfully in a finite number of trials. A backtracking scheme is described in [20]. Moreover, global convergence is also established in [20]. Indeed, if the symmetric part of the Jacobian of F at any x_k is positive (or negative) definite for all k, then the sequence $\{f(x_k)\}$ tends to zero.

2.3 Inverse Preconditioning schemes

We will adapt the recent work by Chehab and Raydan [9] for approximating the Newtons's direction using an Ordinary Differential Equation (ODE) model, to the nonlinear system (1) within the framework of the iterative global preconditioned residual algorithm of the previous subsection. For that, we develop an automatic and implicit scheme to approximate directly the preconditioned direction d_k at every iteration, without an *a priori* knowledge of the Jacobian of F, and involving only a reduced and controlled amount of storage and computational cost. As we will discuss later, this new scheme avoids as much as possible the cost of any calculations involving matrices, and will also allow us to obtain asymptotically the Newton's direction by improving the accuracy in the ODE solver.

The method we introduce here starts from the numerical integration of the Newton flow aimed at computing the root of F as the stable steady state of

$$\frac{dx}{dt} = -(\nabla F(x))^{-1}F(x). \tag{9}$$

The value $\|F(x)\|$ is decreasing along the integral curves and converges at an exponential rate to the root of F. Introducing the decoupling

$$\frac{dx}{dt} = -z \tag{10}$$

$$(\nabla F(x))z = F(x) \tag{11}$$

we see that the algebraic condition that links z to x is in fact a preconditioning equation. In order to relax its resolution, a time derivative in z is added as

$$\frac{dx}{dt} = -z \tag{12}$$

$$\epsilon\frac{dz}{dt} = F(x) - \nabla F(x)z \tag{13}$$

Here $\epsilon > 0$ is a given parameter, generally chosen to be equal to 1. This last system allows to compute numerically the root of F by an explicit time marching scheme since the steady state is asymptotically stable, see [9] for more details. Let t_k be discrete times, we denote by $x_k \simeq x(t_k)$ and by $z_k \simeq z(t_k)$. The application of the simple forward Euler method to (12) reads

$$x^{k+1} = x^k + (t_{k+1} - t_k) z_k \tag{14}$$

$$z^{k+1} = z^k + \frac{(t_{k+1} - t_k)}{\epsilon} \left(F(x^k) - \nabla F(x^k) z^k \right). \tag{15}$$

Remark 1 *As stated above, we want to avoid the computation of the Jacobian matrix, so $\nabla F(x)z$ is classically approached by a finite difference scheme*

$$\nabla F(x) z \simeq \frac{F(x + \tau z) - F(x)}{\tau}$$

for a small given real number τ.

Notice that the dynamics of the differential system (12) can be very slow and, as proposed in [9], a way to speed-up the convergence to the steady state is to introduce artificially two scales in time by computing for every discrete time t_k an approximation of the steady state of the equation in z. More precisely we write

`Step 1- With optimization method 1, compute` z^k `as the approximation of the steady state of`	$\epsilon \frac{dz}{dt} = F(x^k) - \frac{F(x^k + \tau z) - F(x^k)}{\tau}$, $z(0) = z^{k-1}$.
`Step 2- With optimization method 2 compute` x^{k+1} `from` x^k `by`	$x^{k+1} = x^k + \alpha_k z_k$

The preconditioning lies on the accuracy for solving step 1. As optimization method #1 we proposed in [9] to apply some iteration of Cauchy-like schemes that we describe in the annex. As optimization scheme # 2, that defines the time step $\alpha_k = t_{k+1} - t_k$, we used the spectral gradient method. Promising results were obtained on some classical optimization problems. However, the resolution of steady NSE necessitates a more robust scheme for the time marching of x^k. The globalized scheme GPR described above becomes crucial in the practical cases. We now present the general form of the scheme

`Implicit GPR Method (IGPR)`

`Step 1- With Cauchy-like minimization, compute` z^k `as the approximation of the steady state of`	$\epsilon \frac{dz}{dt} = F(x^k) - \frac{F(x^k + \tau z) - F(x^k)}{\tau}$, $z(0) = z^{k-1}$.
`Step 2- with GPR compute` x^{k+1} `from` x^k `by`	$x^{k+1} = x^k + \alpha_k z_k$

3 IGPR method for solving the Steady 2D lid driven cavity

3.1 The problem

The equilibrium state of a driven square cavity is described by the steady Navier-Stokes which, in primary variables, read

$$\begin{aligned} -\frac{1}{\text{Re}} \Delta U + \nabla P + (U \cdot \nabla U) &= f \text{ in } \Omega =]0,1[^2, \\ \nabla \cdot U &= 0, \text{ in } \Omega =]0,1[^2, \\ U &= g, \text{ on } \partial\Omega. \end{aligned} \tag{16}$$

Here $U = (u, v)$ is the velocity field, P is the pressure and f is the external force. For our applications we will consider the so-called driven cavity case so $f = 0$ and the fluid is driven by a proper boundary condition. We denote by $\Gamma_i \;\; i = 1, .., 4$ the sides of the unit square Ω as follows: Γ_1 is the lower horizontal side, Γ_3 is the upper horizontal side, Γ_2 is the left vertical side, and Γ_4 is the right vertical side.

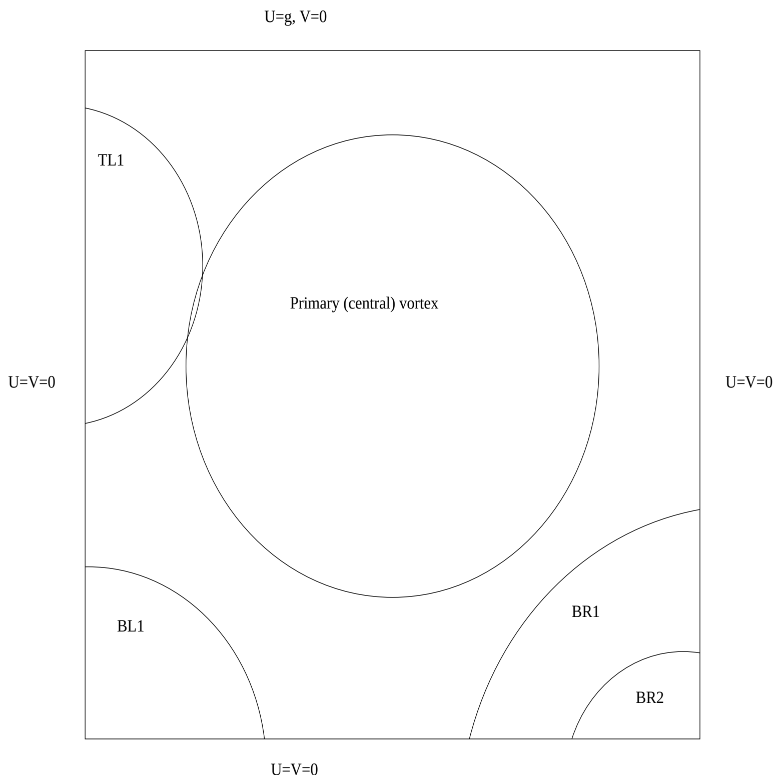

Figure 1: The lid driven cavity - Schematic localization of the mean vortex regions

We distinguish two different driven flow, according to the choice of the boundary conditions on the velocity. More precisely we have

- $g(x) = 1$: Cavity A (lid driven cavity)
- $g(x) = (1 - (1 - 2x)^2)^2$: Cavity B (regularized lid driven cavity)

Anyway, as described bellow, we shall rewrite the driven cavity test problem in terms of stream function and vorticity.

3.2 Discretization and implementation in primary variable

3.2.1 Discretization

The discretization is performed on staggered grids of MAC type in order to verify a discrete Inf-Sup (or Babushka-Brezzi) condition which guarantees the stability, see [23].
Taking N discretization points on each direction of the Pressure grid, we obtain the linear system

$$\left\{ \begin{array}{l} \nu A_u U + B_x P + NL_u(U, V) - F1 = 0 \\ \nu A_v V + B_y P + NL_v(U, V) - F2 = 0 \\ B_x^t U + B_v^t V = 0 \end{array} \right. \tag{17}$$

where $U, V \;\in \mathbb{R}^{N(N-1)}$, $P \in \mathbb{R}^{N\times N}$. (17) is then a square linear system of $2 \times N(N-1) + N^2$ unknowns.

3.2.2 Implementation

The discrete problem reads

$$\left\{\begin{array}{l}\nu A_u U + B_x P + NL_u(U,V) - F1 = 0\\ \nu A_v V + B_y P + NL_v(U,V) - F2 = 0\\ B_x^t U + B_v^t V = 0\end{array}\right. \tag{18}$$

or equivalently

$$\mathcal{F}(U,V,P) = 0,$$

with the obvious notation.

Now, let $\mathcal{S}$ be the Stokes solution operator defined by

$$\mathcal{S}(F,G,0) \mapsto (U,V,P)$$

where (U,V,P) is solution of the Stokes problem

$$\left\{\begin{array}{l}\nu A_u U + B_x P = F\\ \nu A_v V + B_y P = G\\ B_x^t U + B_v^t V = 0\end{array}\right. \tag{19}$$

Let us introduce the functional $\mathcal{G}$

$$\mathcal{G}((U,V,P) = \mathcal{S}(\mathcal{F}(U,V,P))$$

The scheme consists in applying the dynamical preconditioned spectral method to the differential system

$$\left\{\begin{array}{l}\dfrac{dX}{dt} = -Z,\\ \epsilon\dfrac{dZ}{dt} = \mathcal{G}(X) - \mathcal{H}Z\end{array}\right. \tag{20}$$

where $X = (U,V,P)$ and where $\mathcal{H}$ is an approximation of the gradient of $\mathcal{G}(X)$.

3.3 The $\omega - \psi$ formulation

One of the advantage of the $\omega - \psi$ formulation is that the NSE are decoupled into two problems: a convection diffusion equation and a Poisson problem. In particular we can use the FFT for solving the linear problems, as pointed out hereafter.

3.3.1 The formulation

The $\omega - \psi$ is obtained by taking the curl of the NSE [14, 23]. Letting $\omega = \dfrac{\partial u}{\partial y} - \dfrac{\partial v}{\partial x}$ and $u = \dfrac{\partial \psi}{\partial y}$, $v = -\dfrac{\partial \psi}{\partial x}$ hence $\Delta\psi = \omega$. We have the equations

$$-\frac{1}{Re}\Delta\omega + \frac{\partial\phi}{\partial y}\frac{\partial\omega}{\partial x} - \frac{\partial\phi}{\partial x}\frac{\partial\omega}{\partial y} = 0 \tag{21}$$

$$\Delta\psi = \omega \tag{22}$$

$$\omega(x,0) = \omega_0(x) \tag{23}$$

The boundary conditions on ω are derived by the discretization of $\Delta\psi$ on the boundaries. With the conditions on u and v we have

$$\begin{array}{ll}\omega(x,0,t) = \dfrac{\partial^2\psi}{\partial y^2}(x,0,t) & \text{on } \Gamma_1\\ \omega(x,1,t) = \dfrac{\partial^2\psi}{\partial y^2}(x,1,t) & \text{on } \Gamma_3\\ \omega(0,y,t) = \dfrac{\partial^2\psi}{\partial x^2}(0,y,t) & \text{on } \Gamma_2\\ \omega(1,y,t) = \dfrac{\partial^2\psi}{\partial x^2}(1,y,t) & \text{on } \Gamma_4\end{array}$$

So, since $\psi_{\partial\Omega} = 0$ and $u = \dfrac{\partial\psi}{\partial y}$, $v = -\dfrac{\partial\psi}{\partial x}$, we obtain by using Taylor expansions

$$\begin{aligned}
\omega_{i,0} &= \frac{\psi_{i,1} - 8\psi_{i,2}}{2h^2} \\
\omega_{i,N+1} &= \frac{-\psi_{i,N-1} + 8\psi_{i,N} - 6h\beta(ih)}{2h^2} \\
\omega_{0,j} &= \frac{\psi_{1,j} - 8\psi_{2,j}}{2h^2} i \\
\omega_{N+1,j} &= \frac{-\psi_{N-1,j} + 8\psi_{N,j}}{2h^2}
\end{aligned} \tag{24}$$

Here $\beta(x)$ denotes the boundary condition function for the horizontal velocity at the boundary Γ_3.
The boundary conditions on ψ are homogeneous Dirichlet BC. l operators are discretized by second order centered schemes on a uniform mesh composed by N points in each direction of the domain of step-size $h = \dfrac{1}{N+1}$. The total number of unknowns is then $2N^2$.
The boundary conditions on ω are iteratively implemented according to the relations (24-24), making the finite differences scheme second order accurate.

3.3.2 Implementation

With the formulae (24-24) we can compute the boundary condition of ω. We denote by $\partial_x^h(\psi)$, $\partial_y^h(\psi)$ and by $\partial_\Delta^h(\psi)$ the contributions of the boundary conditions to the discretization operators of ∂_x, ∂_y and $-\Delta$. The problem to solve reads

$$F_1(\omega,\psi) = \frac{1}{Re}\left(A\omega + \partial_\Delta^h(\psi)\right) + D_y\psi\left(D_x\omega + \partial_x^h(\psi)\right) - D_x\psi\left(D_y\omega + \partial_y^h(\psi)\right) = 0, \tag{25}$$

$$F_2(\omega,\psi) = A\psi + \omega = 0 \tag{26}$$

Here A is the discretization matrix of $-\Delta$, D_x and D_y are the discretization matrices of ∂_x and ∂_y respectively. The problem to solve is then

$$F(\omega,\psi) = \begin{pmatrix} F_1(\omega,\psi) \\ F_2(\omega,\psi) \end{pmatrix} = \begin{pmatrix} 0 \\ 0 \end{pmatrix}$$

We set for convenience $X = (\omega, \psi)$. Now, as for the primary variables formulation and returning to the dynamical system framework of the method, we set

$$\mathcal{G}(\omega,\psi) = \begin{pmatrix} A^{-1}F_1(\omega,\psi) \\ A^{-1}F_2(\omega,\psi) \end{pmatrix}$$

and we consider the evolutionary system

$$\left\{\begin{array}{l} \dfrac{dX}{dt} = -Z, \\ \epsilon\dfrac{dZ}{dt} = \mathcal{G}(X) - \mathcal{H}Z \end{array}\right. \tag{27}$$

where $\mathcal{H}Z$ is an approximation of the gradient of $\mathcal{G}(X)$ at Z.

Here A is the classical pentadiagonal finite differences matrix of the Laplace operator on a square and the solution of linear systems with A can be cheaply done by using fast solvers such as FFT or multigrid. We will use in this paper the FFT.

4 Numerical results

4.1 General implementation of the algorithm

We now list the information (data) required by the method:

- The number M.
- The parameters γ and η_k (that we will set to 0).
- The initial value of the descent parameter α_0.
- The merit function. We use the Euclidian norm of the residual $\|F(X)\|$.
- The accuracy of the global method: the solution is considered as accurate enough when $\|F(X)\| < 1.e-6$.
- The accuracy imposed for solving the preconditioning equation

$$\frac{F(x^k + \tau z) - F(x^k)}{\tau} - F(x^k) = 0,$$

  that is characterized by

  - the choice of the optimization method #1. We will use Enhanced Cauchy 2 as presented in the annex
  - the number τ. We set $\tau = 1.e-8$
  - the number of iteration $nprec$ that can vary at each step. We choose to increase $nprec$ as the residual r^k decreases for improving the preconditioning near the solution as follows (adaptive preconditioning)

`adaptive computation of nprec`

$nprec0$ given
for $k = 0, \cdots$ (until convergence)
if $\|r^k\| < 1.e-1$
$nprec = ceil * (-log_{10}(\|r^k\|) + 1) * nprec0$

4.2 Computation of Steady states of NSE

We present hereafter the numerical solution of the steady state of the bi-dimensional driven cavity for different Reynolds numbers. Our results agree with those in the literature [6, 4, 13, 16, 17, 22, 26, 27, 28](see figures and tables below) and to prove the robustness of the resolution method, we take as initial guess the solution of the Stokes problem which becomes farther from the steady state as the Reynolds number increases. In here we pay special attention on the solution of NSE in the $\omega - \Psi$ formulation. However let us mention that the scheme applies also to NSE in primary variables $(U - P)$, the linear solver being a Stokes solver (see annex). The crucial practical point is to have at the disposal a fast solver for the linear problems: FFT or multigrid for $\omega - \Psi$ formulation and Multigrid Uzawa [6] for the $U - P$ formulation.

As pointed out in the following results, the globalization strategy is important while the residual is not small enough. Furthermore, the preconditioning makes sense "close to the solution". For that reason we choose to activate the preconditioning progressively as the residual decreases by increasing the number of inner iterations in the solution of the preconditioning step (step 1 of the scheme). This allows us to obtain a fast convergence at the end while saving computational time at the beginning.

We observe that the number of outer iterations increases with the Reynolds number but not so much with the dimension of the problem. In all cases, the first part of the convergence process is devoted to "maintaining" the iterates in a neighborhood of the solution.
All the computations have been made using Matlab © software on a 2Ghz dual core PC with 2 ram's Gbytes.

4.3 Cavity B

We now present the parameters of the scheme that we used for solving the flow in cavity B for the stream function-vorticity formulation of NSE. N is the number of discretization point in each direction of the domain.

4.3.1 Re=1000

$N = 127, \gamma = cste = 9.10^2, M = 2, nprec0 = 4, method = Enhanced\ Cauchy\ 2, nprec = adapt, \alpha_0 = 1.e1$

4.3.2 Re=2000

$N = 127, \gamma = cste = 9.10^1 1, M = 2, nprec0 = 4, method = Enhanced\ Cauchy\ 2, nprec = adapt, \alpha_0 = 1.e4$

4.3.3 Re=5000

$N = 255, \gamma = cste = 9.10^2, M = 2, nprec0 = 4, method = Enhanced\ Cauchy\ 2, nprec = adapt, \alpha_0 = 1.e1$

4.4 Cavity A

4.4.1 Re=1000

$N = 127, \gamma = cste = 9.10^2, M = 2, nprec0 = 4, method = Enhanced\ Cauchy\ 2, nprec = adapt, \alpha_0 = 1.e1$

4.4.2 Re=3200

$N = 255, \gamma = cste = 9.10^6, M = 2, nprec0 = 5, method = Enhanced\ Cauchy\ 2, nprec = adapt, \alpha_0 = 1.e4$

The results are reported on figure 2 to 4 and special values of the solution are given in tables 1, 2, and 3 where we also compare them with those in the literature.

We note that the main effort of the iterative method is done at the beginning of the iterations, the globalization acting to stabilize the iterates. This phenomenon is amplified as the Reynolds number Re becomes large. An acceleration of the convergence is obtained when the residual is small enough since $nprec$ increases. The shape of the solutions are identical with that of all the publications to which we refer and the special values agree, see tables 1, 2, and 3.

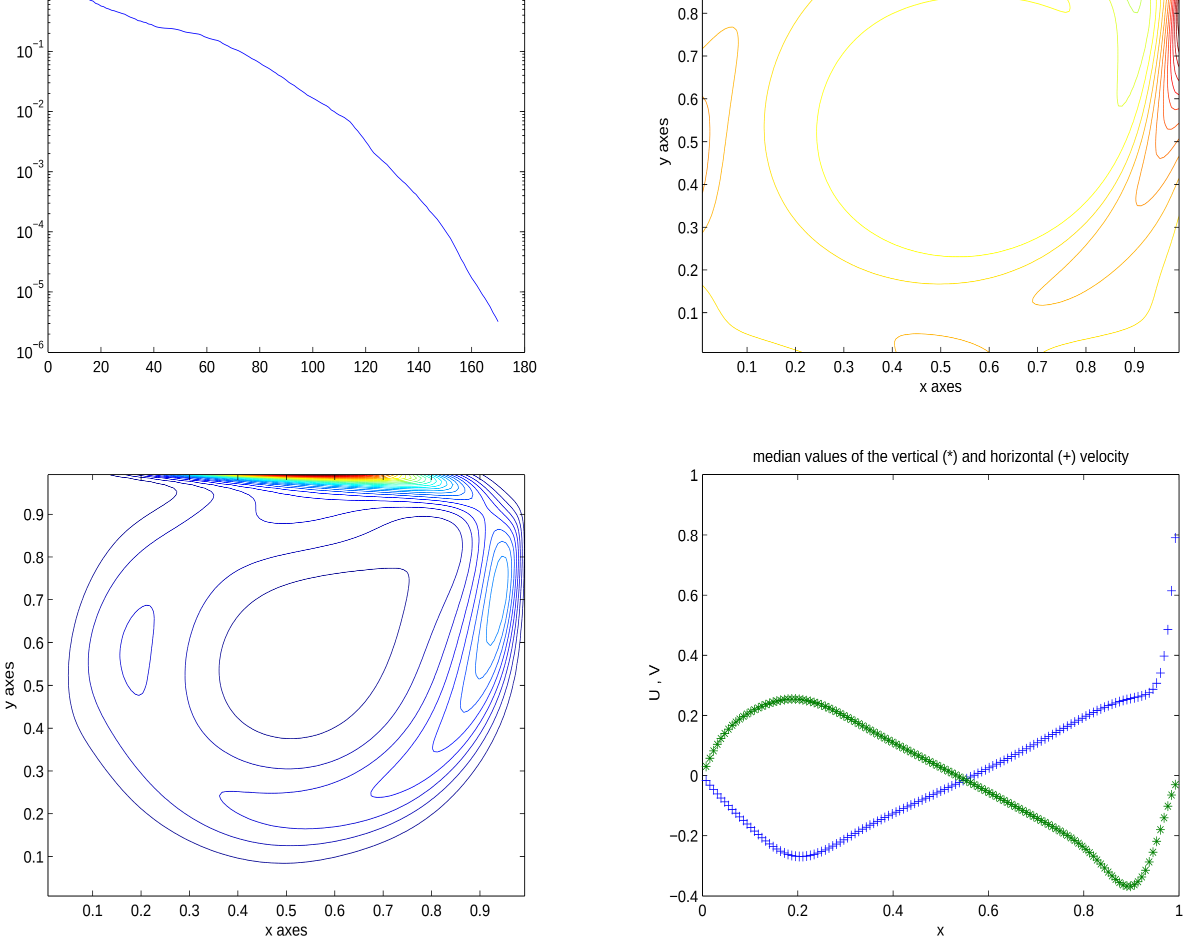

Figure 2: Steady NSE, Re=1000, N=127. Residual vs iterations, median values of the horizontal and of the vertical velocity ; Isolines of the kinetic energy and of the vorticity

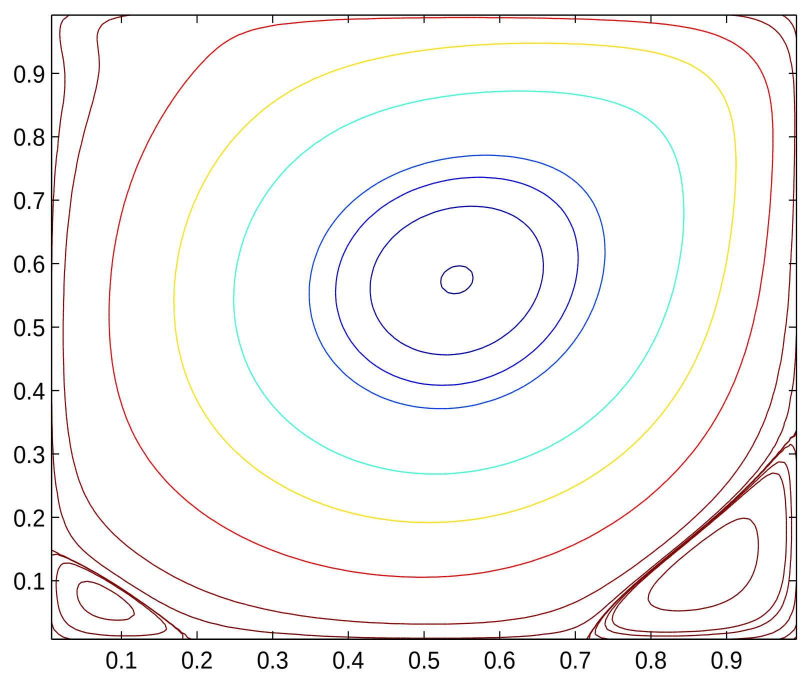

Figure 3: Steady NSE, Cavity B, Re=1000, N=127. Isolines of the stream function

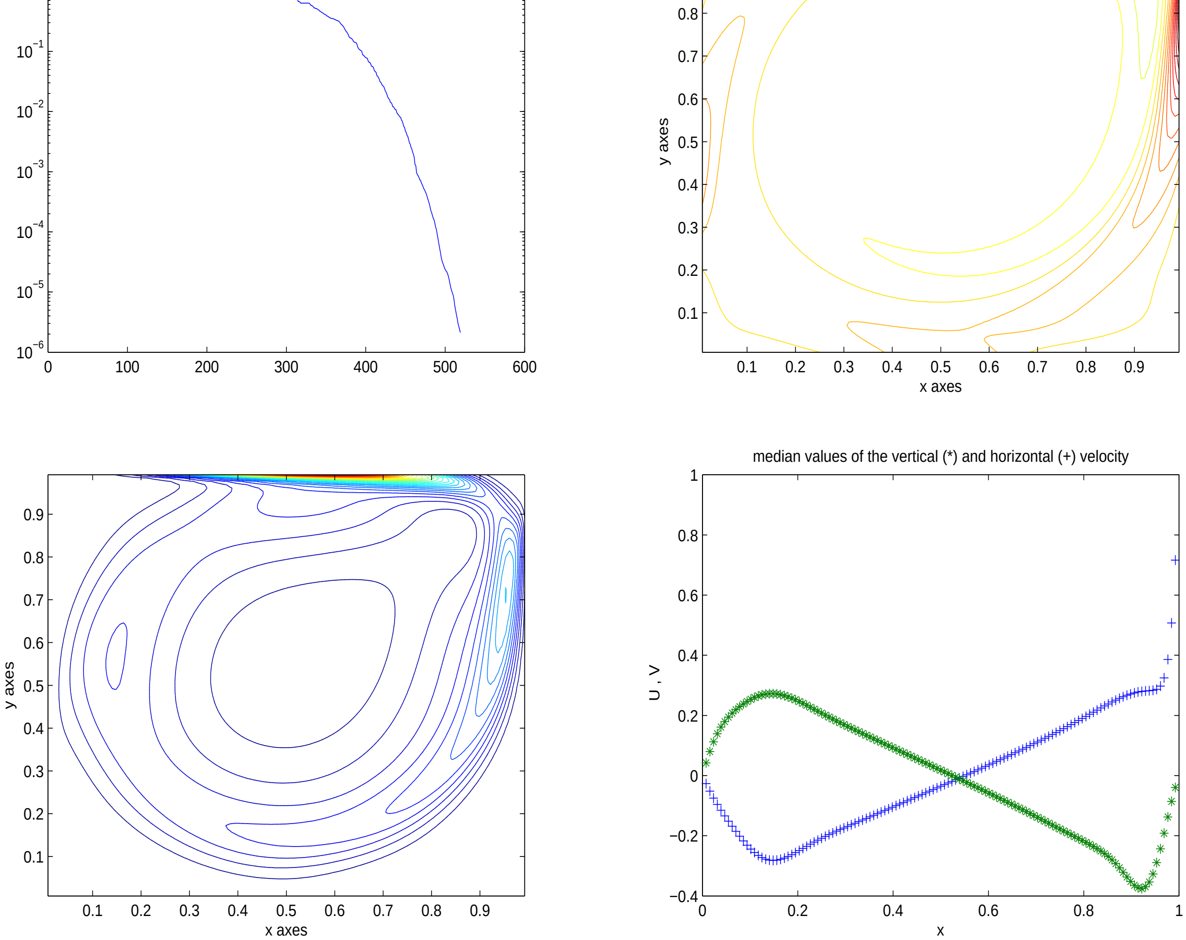

Figure 4: Steady NSE, Re=2000, N=127. Residual vs iterations, median values of the horizontal and of the vertical velocity ; Isolines of the kinetic energy and of the vorticity

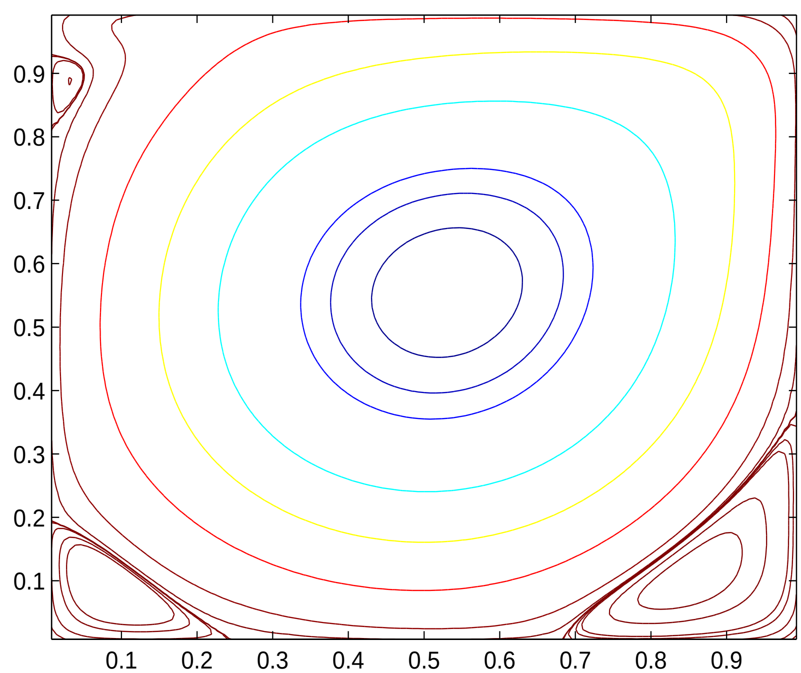

Figure 5: Steady NSE, Cavity B, Re=2000, N=127 . Isolines of the stream function

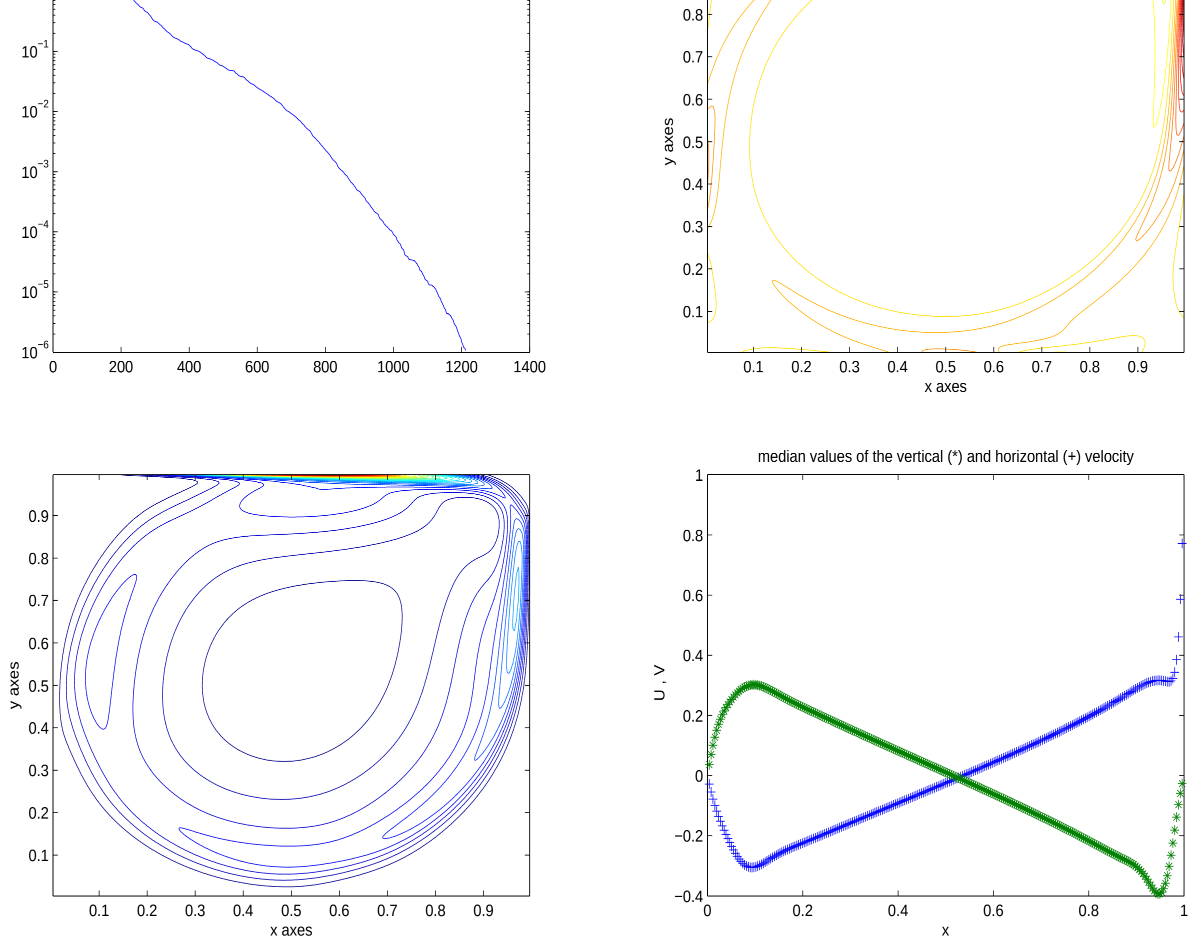

Figure 6: Steady NSE, Re=5000, N=255. Residual vs iterations, median values of the horizontal and of the vertical velocity ; Isolines of the kinetic energy and of the vorticity

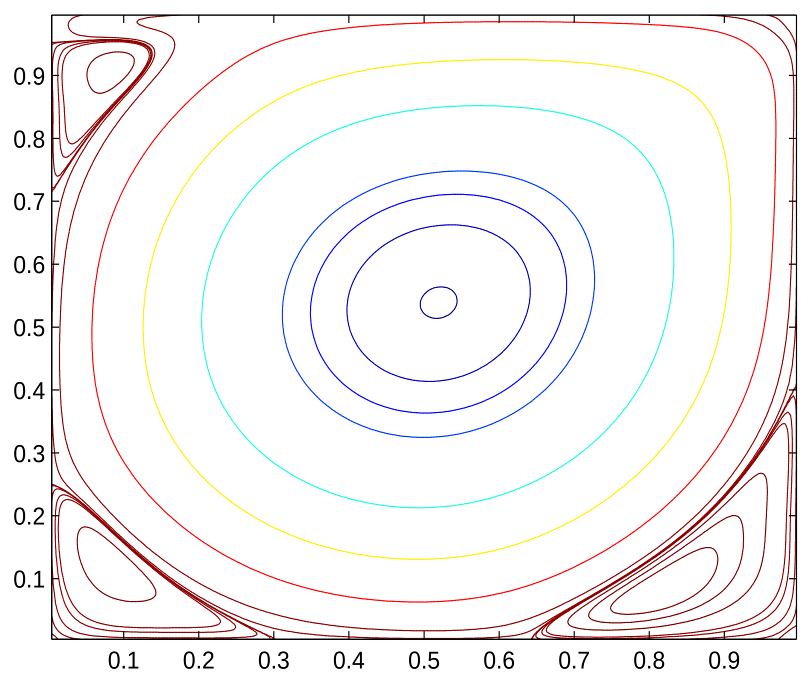

Figure 7: Steady NSE, Cavity B, Re=5000, N=255 isolines of the stream function

Table 1: Cavity B. Re=1000

	IGPR	IGPR	Pascal [22]	Pascal [22]	Shen [26]	Shen [26]
Formulation	$\omega - \psi$	$\omega - \psi$	U, P	U, P	U, P	U, P
Discretization x	FD	FD	FEM	FEM	Spectral	Spectral
Grid/Mesh	127x127	63x63	65x65	129x129	64x64	25x25
Δt			0.1	0.05		0.15
Vortex						
x	0.5469	0.5469	0.5469	0.5547	0.5469	0.547
y	0.5781	0.5781	0.5781	0.5859	0.5781	0.578
ψ	-0.08517	-0.07982	-0.09220	-0.09028	-0.0843	-0.08717
ω	-1.57363	-1.4930	-1.944	-2.168		
Vortex (B L)						
x	0.078	0.0781	0.0625	0.0547	0.08	0.078
y	0.0625	0.0625	0.0625	0.0547	0.09	0.063
ψ	$0.7544\ 10^{-4}$	0.586110^{-4}	$0.315\ 10^{-4}$	$0.127\ 10^{-4}$	$0.515\ 10^{-4}$	$0.828\ 10^{-4}$
ω	0.13	0.1160	0.0761	0.048		
Vortex (B R)						
x	0.867	0.875	0.875	0.867	–	0.922
y	0.1171	0.125	0.125	0.125	–	0.094
ψ	$0.9452\ 10^{-3}$	$0.83617\ 10^{-3}$	$0.922\ 10^{-3}$	$0.855\ 10^{-3}$	$0.882\ 10^{-3}$	$0.568\ 10^{-3}$
ω	0.60138	0.5825	0.6069	0.5099		

Table 2: Cavity B. Re=2000

	IGPR	Shen [26]	Shen [26]
Formulation Discretization x Grid / Mesh Δt	$\omega - \psi$ FD 127x127	$\omega - \psi$ Spectral 33x33	$\omega - \psi$ Spectral 25x25
Vortex			
x	0.5312	0.516	0.531
y	0.5546	0.547	0.547
ψ	-0.08361	-0.08776	-0.08762
ω	-1.4370		
Vortex (B L)			
x	0.08593	0.094	0.078
y	0.09375	0.094	0.094
ψ	$3.1435\ 10^{-4}$	$3.5432\ 10^{-4}$	$3.1772\ 10^{-4}$
ω	0.3862		
Vortex (B R)			
x	0.8515	0.922	0.922
y	0.1015	0.094	0.094
ψ	$1.495\ 10^{-3}$	$0.80841\ 10^{-3}$	$0.80667\ 10^{-3}$
ω	0.9448		
Vortex (U L)			
x	0.03125	0.031	0.031
y	0.8906	0.92	0.92
ψ	$5.1499\ 10^{-5}$	1.449710^{-5}	1.714310^{-5}
ω	0.3051		

Table 3: Cavity B. Re=5000

	IGPR	IGPR	Shen [27]	Pascal [22]
Formulation	$\omega - \psi$	$\omega - \psi$	U, P	U, P
Discretization x	FD	FD	Spectral	FEM
Grid / Mesh	127x127	255x255	33x33	129x129
Δt			0.03	0.05
Vortex				
x	0.5234	0.51953	0.516	0.5390
y	0.539	0.539	0.531	0.5313
ψ	-0.07761	-0.085211	-0.08776	-0.0975
ω	-1.2687	-1.3866		-2.169
Vortex (B L)				
x	0.078125	0.78125	0.094	0.0859
y	0.125	0.125	0.094	0.1172
ψ	$6.8393\ 10^{-4}$	7.9510^{-4}	$7.5268\ 10^{-4}$	6.72310^{-4}
ω	0.7468	0.844		0.7310
Vortex (B R)				
x	0.8203	0.8164	0.922	0.8047
y	0.08593	0.082	0.094	0.0781
ψ	$1.8528\ 10^{-3}$	2.04110^{-3}	$0.77475\ 10^{-3}$	$2.42\ 10^{-3}$
ω	1.42177	1.58687		2.009
Vortex (U L)				
x	0.07812	0.0859	0.078	0.0781
y	0.9062	0.9101	0.92	0.906
ψ	$5.6645\ 10^{-4}$	7.14910^{-4}	6.77810^{-4}	$7.86\ 10^{-4}$
ω	0.88813	1.098		1.159

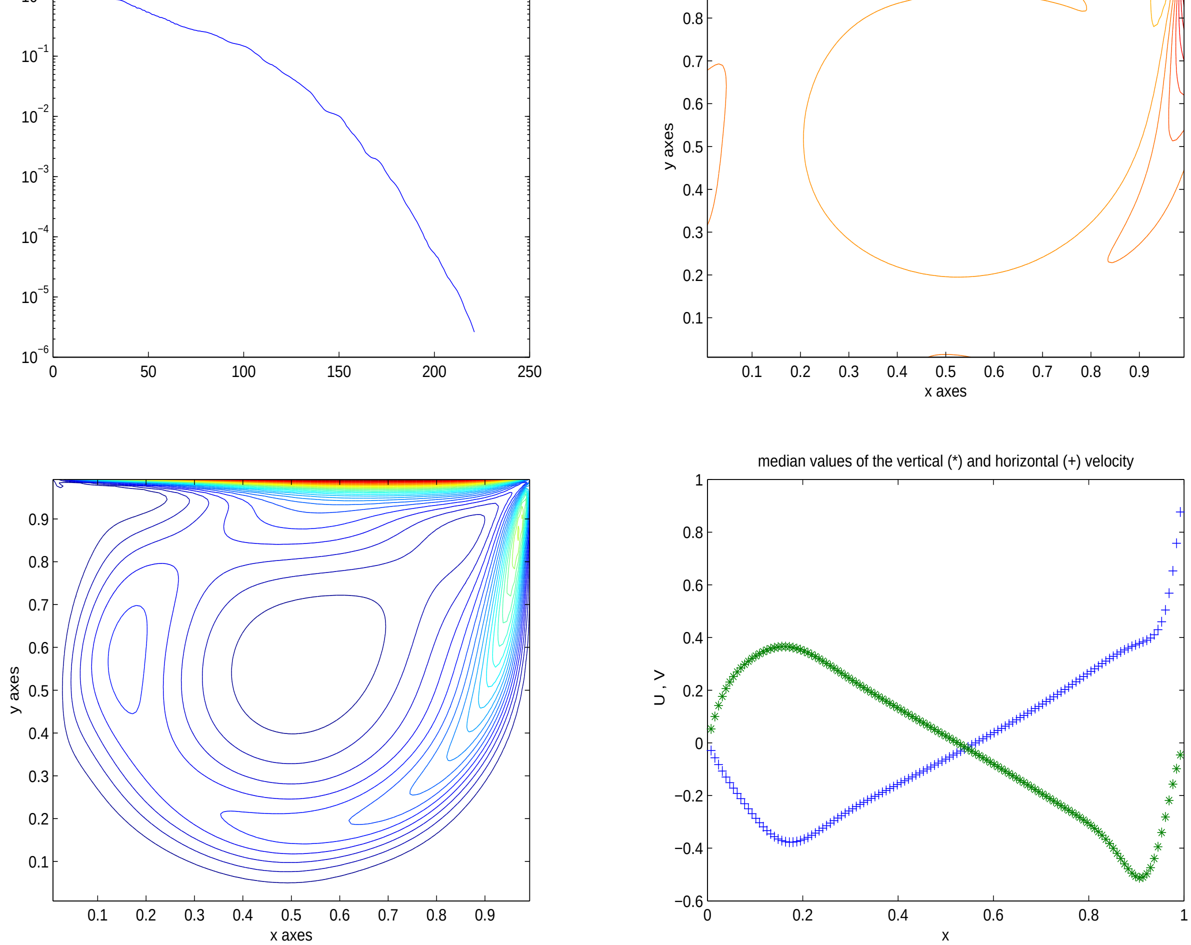

Figure 8: Steady NSE, Re=1000, N=127. Residual vs iterations, median values of the horizontal and of the vertical velocity ; Isolines of the kinetic energy and of the vorticity

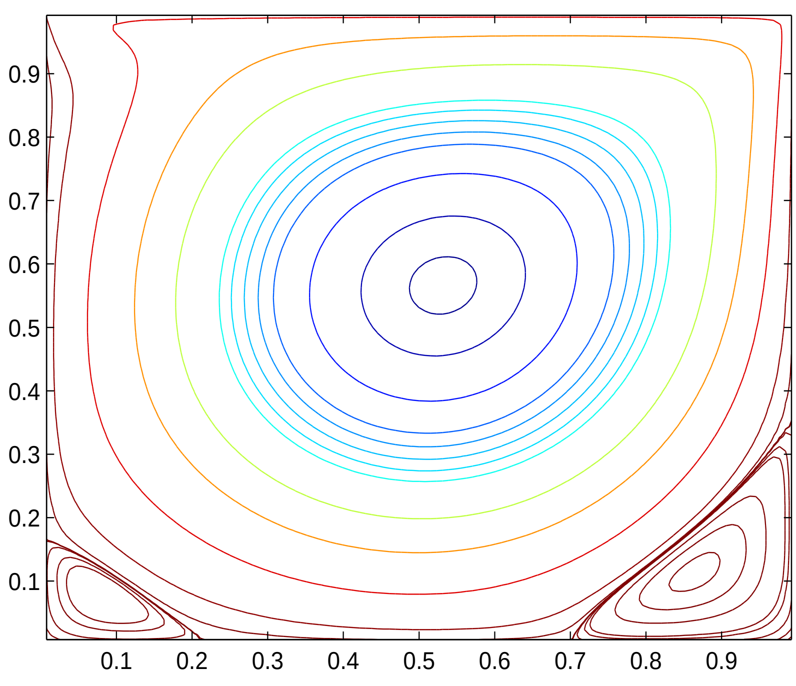

Figure 9: Steady NSE, Cavity A, Re=1000, N=127. Isolines of the stream function

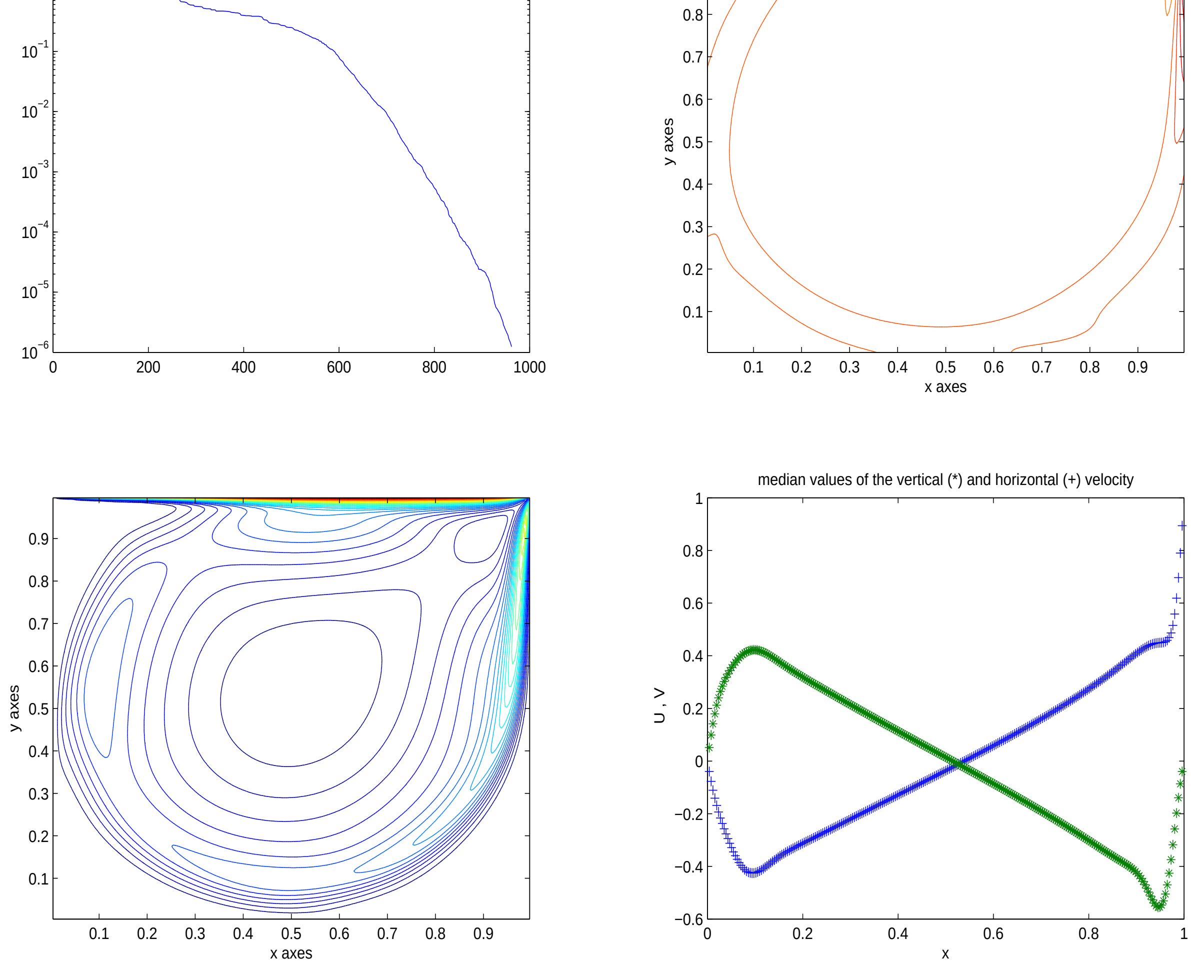

Figure 10: Steady NSE, Re=3200, N=255. Residual vs iterations, median values of the horizontal and of the vertical velocity ; Isolines of the kinetic energy and of the vorticity

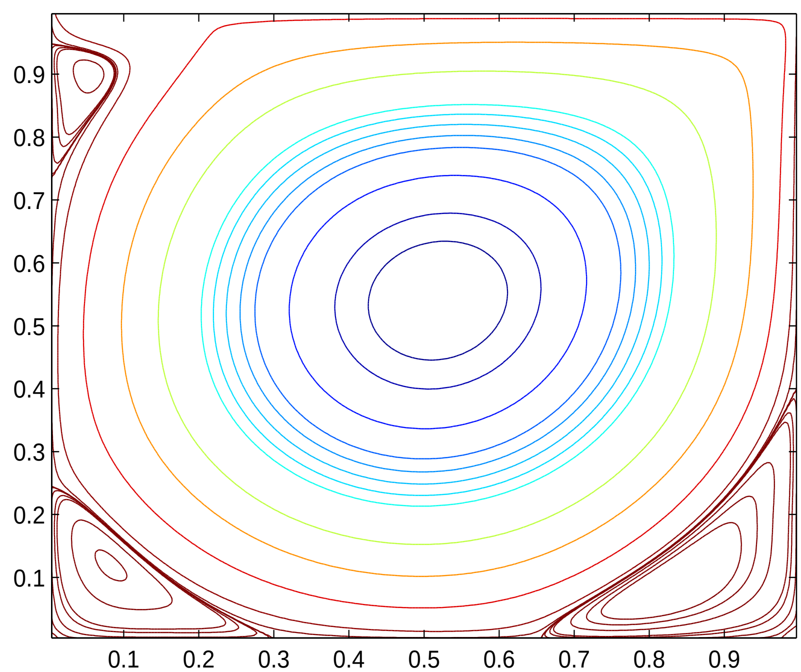

Figure 11: Steady NSE, Cavity A, Re=3200, N=255. Isolines of the stream function

Table 4: Cavity A. Re=1000

	IGPR	Pascal [22]	Bruneau / Jouron [6]	Goyon[17]	Sonke [28]
Formulation	$\omega - \psi$	U, P	U, P	$\omega - \psi$	U ω
	stat.	evol.	Multigrid	evol.	evol
Discretization x	FD	FEM	FD	FD	FEM
Grid/Mesh	127x127	65x65	129x129	64x64	120x120
Δt		0.1			
Vortex					
x	0.5313	0.5313	0.5313	0.5312	0.5368
y	0.5625	0.5625	0.5586	0.5625	0.5693
ψ	-0.116008	-0.1231	-0.1163	-0.1157	-0.1210
ω	-2.025	-2.185			
Vortex (B L)					
x	0.0859	0.078	0.0859	0.0859	0.0834
y	0.0781	0.078	0.0820	0.0781	0.0637
ψ	$2.1303 10^{-4}$	$2.28\ 10^{-4}$	$3.25\ 10^{-4}$	$2.11\ 10^{-4}$	$2.74\ 10^{-4}$
ω		0.3242			
Vortex (B R)					
x	0.8671	0.875	0.8711	0.867	0.8513
y	0.1171	0.125	0.1094	0.1171	0.1237
ψ	$1.66\ 10^{-3}$	$1.69\ 10^{-3}$	$1.91\ 10^{-3}$	$1.63\ 10^{-3}$	$3.01\ 10^{-2}$
ω	1.08	1.29			

Table 5: Cavity A. Re=3200

	IGPR	Ghia [16]	Bruneau / Jouron [6]	Goyon [17]	Croisille [4]
Formulation	$\omega - \psi$	U, P	U, P	$\omega - \psi$	U ω
	stat.	Multigrid	Multigrid	evol.	evol
Discretization x	FD	FD	Gal. Class	Gal. Class	Gal. Class
Mesh	255x255	255x255	129x129	64x64	120x120
Δt					
Vortex					
x	0.51953	0.5165	0.5313	0.5312	0.5368
y	0.539	0.5469	0.5586	0.5625	0.5693
ψ	-1.1917	-0.1203	-0.1163	-0.1157	-0.1210
ω	-1.921	-2.185			
Vortex (B L)					
x	0.082	0.078	0.0859	0.0859	0.0834
y	0.1211	0.078	0.0820	0.1171	0.0637
ψ	1.07810^{-3}	$9.78\ 10^{-4}$	$3.25\ 10^{-4}$	$9.93\ 10^{-4}$	$2.74\ 10^{-4}$
ω	1.168				
Vortex (B R)					
x	0.8281	0.8125	0.8711	0.867	0.8513
y	0.0859	0.0859	0.1094	0.1171	0.1237
ψ	2.7710^{-3}	$3.13\ 10^{-3}$	$1.91\ 10^{-3}$	$2.62\ 10^{-3}$	$3.01\ 10^{-2}$
ω	2.29				
Vortex (U L)					
x	0.05468	0.0546	0.8711	0.0546	0.8513
y	0.9023	0.8984	0.1094	0.9062	0.1237
ψ	$6.93\ 10^{-4}$	$7.27\ 10^{-4}$		$6.38\ 10^{-4}$	$3.01\ 10^{-2}$
ω	1.7053	1.29			

5 Concluding remarks

We have presented a scheme that takes into account only the linear part of the equation for solving steady fluid flows, making our method a very general one. The efficiency of the scheme is increased when a fast solver is used for the linear problem. The results we obtain on the numerical solution of NSE show that the proposed method is robust; as it has been already established, it is harder to solve directly the steady NSE than to compute the steady state by time marching schemes applied to the evolutionary equation. The new method is also flexible since the choice of the preconditioning step is completely free. We would like to stress out that the preconditioned globalized spectral gradient method can be applied in a large number of situation and fields, especially when no (simple) preconditioning can be built, such as in CFD, and also in numerical linear algebra when solving Riccati matrix equations or for some other nonlinear matrix problems. This is a topic that deserves further investigation.

Acknowledgements *This work was supported by SIMPAF project from INRIA futurs.*

References

[1] J. Barzilai and J. M. Borwein (1988). Two-point step size gradient methods, *IMA Journal of Numerical Analysis*, 8, 141–148.

[2] P. Brown, and Y. Saad (1990). Hybrid Krylov methods for nonlinear systems of equations, *SIAM Journal on Scientific Computing 11*, 450–481.

[3] P. Brown, and Y. Saad (1994). Convergence theory of nonlinear Newton-Krylov algorithms, *SIAM Journal on Optimization 4*, 297–330.

[4] M. Ben-Artzi, J.-P. Croisille, D. Fishelov and S. Trachtenberg (2005). A pure-compact scheme for the streamfunction formulation of Navier-Stokes equations, *Journal Comp. Phys.*, 205 (2005), no 2, 640–664.

[5] C. Brezinski, J.-P. Chehab, Nonlinear hybrid procedures and fixed point iterations, Num. Func. Anal. Opt., 19 (1998), 465-487.

[6] C.-H. Bruneau and C. Jouron (1990). An efficient Scheme for solving Steady incompressible Navier-STokes equations, *Journal Comp. Phys.* 89, 389–413.

[7] A. Cauchy [1847], Méthodes générales pour la résolution des systèmes d'équations simultanées, *C. R. Acad. Sci. Par.* 25, pp. 536–538.

[8] J.-P. Chehab and J. Laminie, Differential equations and solution of linear systems, Numerical Algorithms (2005), 40, 103-124.

[9] J.-P. Chehab and M. Raydan (2005). Inverse and adaptive preconditioned gradient methods for nonlinear problems, *Num. Math.* 55, 32–47

[10] M. Crouzeix, *Approximation et méthodes itératives de résolution d'inéquations variationelles et de problèmes non linéaires*, I.R.I.A., cahier 12, Mai 1974, 139-244.

[11] Y. H. Dai and L. Z. Liao (2002). R-linear convergence of the Barzilai and Borwein gradient method, *IMA Journal on Numerical Analysis* 22, pp. 1–10.

[12] J.E. Dennis Jr. and R.B. Schnabel (1983), *Numerical Methods for Unconstrained Optimization and Nonlinear Equations*, Prentice-Hall, Englewood Cliffs, NJ.

[13] E. Erturk, T.C. Corke and C. Gökçöl, Numerical Solutions of 2-D Steady Incompressible Driven Cavity Flow at High Reynolds Numbers, Int. J. Numer. Meth. Fluids 2005, Vol 48, pp 747-774.

[14] D. Euvrard, *Résolution numérique des équations aux dérivées partielles*, Dunod, 350 pp, 1994, 3rd Edition.

[15] R. Fletcher (2005). On the Barzilai-Borwein method. In: *Optimization and Control with Applications* (L.Qi, K. L. Teo, X. Q. Yang, eds.) Springer, 235–256.

[16] U. Ghia, K.N. Ghia and C.T. Shin (1982). High-Re Solutions of incompressible Flow using the Navier-Stokes equations and the multigrid method, *Journal Comp. Phys.* 48, 387–411.

[17] O. Goyon (1996). High-Reynolds Number Solutions of Navier-Stokes Equations using Incremental Unknowns, *Comput. Meth. Appl. Mech. and Eng.* 130, 319–335.

[18] C. T. Kelley (1995). *Iterative Methods for Linear and Nonlinear Equations.* SIAM, Philadelphia.

[19] W. La Cruz and M. Raydan (2003). Nonmonotone Spectral Methods for Large-Scale Nonlinear Systems, *Optimization Methods and Software*, 18, 583–599.

[20] W. La Cruz, J. M. Martínez and M. Raydan (2004). Spectral residual method without gradient information for solving large-scale nonlinear systems, *Math. of Comp.*, to appear.

[21] F. Luengo, M. Raydan, W. Glunt, T.L. Hayden, Preconditioned spectral gradient method, *Numerical Algorithms*, Vol. 30, pp. 241-258, 2002.

[22] F. Pascal, *Méthodes de Galerkin non lináires en discrétisation par éléments finis et pseudo-spectrale. Application à la mécanique des fluides*, Thèse Université Paris XI, Orsay, janvier 1992.

[23] R. Peyret, R. Taylor, *Computational methods for fluid flows*, Springer series in Computational Physics, Springer 1983.

[24] M. Raydan (1993). On the Barzilai and Borwein choice of the steplength for the gradient method, *IMA Journal on Numerical Analysis 13*, 321–326.

[25] M. Raydan (1997). The Barzilai and Borwein gradient method for the large scale unconstrained minimization problem, *SIAM Journal on Optimization*, 7, 26–33.

[26] J. Shen (1990). Numerical simulation of the regularized driven cavity flows at high Reynolds numbers, *Comput. Meth. in Applied Mech. and Eng.* 80, 273–280.

[27] J. Shen (1991). Hopf bifurcation of the Unsteady regularized driven cavity flow, *J. Comput. Phys.* 95, 228–245.

[28] L. Sonke Tabuguia, *Etude numérique des équations des Navier-Stokes en milieux multiplement connexes, en formulation vitesse-tourbillon, par une approche multidomaine* Paris XI, Orsay, 1989.

[29] R. Temam, *Navier Stokes equations*, North Holland, 1984.

[30] S. Turek, *Efficient dsolvers for incompressible flows problems*, Lecture Notes in Computational Science and Engineering, Springer, 1999.

[31] L.B. Zhang, *Un schéma de semi-discrétisation en temps pour des systèmes différentiels discrétisés en espace par la méthode de Fourier. Résolution numérique des équations de Navier-Stokes stationnaires par la méthode multigrille.* Thése, Université Paris–Sud, Orsay, 1987.

6 Annex

6.1 Solution of NSE in primary variables

We present the numerical results on the solution of the steady NSE in primary variables. We change the value of γ during the iterations in order to increase the non-monoticity of the PSG as follows

$$\text{if } \|r^k\| < 1.e-3 \text{ then } \gamma = 0.9$$

We now present the numerical solution of the cavity B problem for $Re = 400$ and $Re = 2000$. The level curves of the pressure, the vorticity, the kinetic energy and the stream function agree with those in the literature. Notice that the number of iterations for convergence are less than the ones needed for the same example but using the stream-vorticity formulation. However the solution of the linear problem requires more effort since the Stokes problem needs to be solved at each evaluation of the nonlinear functional, while the solution of Poisson problems is needed when considering the $\omega - \Psi$ formulation for NSE.

6.1.1 Re=400

$N = 63, \gamma = cste = 9.10^4, M = 2, nprec0 = 5, method = Enhanced\ Cauchy\ 2, nprec = adapt, \alpha_0 = 1.e2$
$\gamma = 0.9\ if\ \|r^k\| < 0.001$

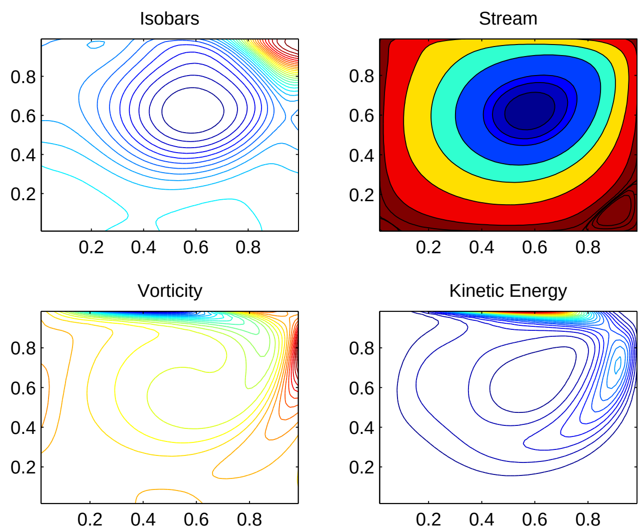

Figure 12: Steady NSE, Cavity B, Re=400, N=63; Isovalues for the streamfunction, the vorticity, the pressure and the kinetic energy

6.1.2 Re=2000

$N = 127, \gamma = cste = 9.10^4, M = 2, nprec0 = 5, method = Enhanced\ Cauchy\ 2, nprec = adapt, \alpha_0 = 1.e2$
$\gamma = 0.9\ if\ \|r^k\| < 0.001$

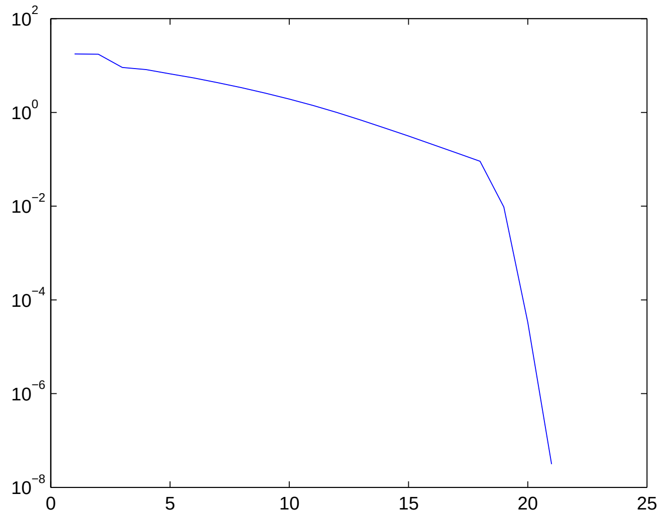

Figure 13: Steady NSE, Cavity B, Re=400, N=63. Residual vs iterations

6.2 Generalized Cauchy methods

6.2.1 Principle

The computation of a steady state by an explicit scheme can be speeded up by enhancing the stability domain of the scheme since it allows to use larger time steps. In that sense the accuracy of a time marching scheme is not a priority. A simple way to derive more stable methods is to use parametrized one-step schemes and to fit the parameters, not for increasing the accuracy such as in the classical schemes (Heun's, Runge Kutta's), but for improving the stability.
For example, in [5, 8] it was proposed a method for computing iteratively fixed points with larger descent parameter starting from a specific numerical time scheme. More precisely, this method consists in integrating the differential equation

$$\begin{cases} \dfrac{dU}{dt} = F(U), \\ \\ U(0) = U_0, \end{cases} \tag{28}$$

by the p- steps scheme

`Given` X_0
`For k=0, ...`
`Set` $K_1 = F(X^k)$
`for m=2,..p`
`set` $K_m = F(x^k + \Delta t K_{m-1})$
`Set` $X^{k+1} = X^k + \Delta t \sum_{i=0}^{p} \alpha_i K_i$

Here $\sum_{i=1}^{p} \alpha_i = 1$.

6.2.2 Minimizing parameters

Classically, the convergence can be speeded-up by computing at each iteration the step-length in order to minimize the Euclidian norm of the current residual: this gives rise to the variant of the Cauchy scheme

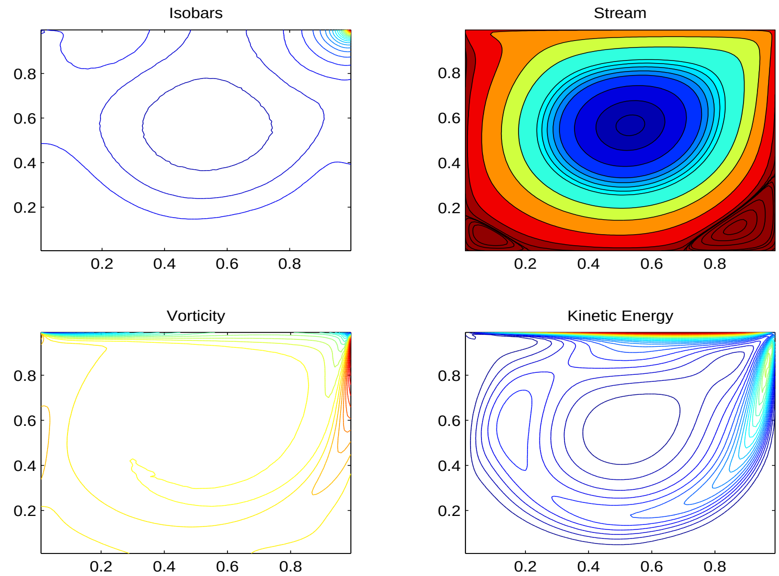

Figure 14: Steady NSE, Cavity B, Re=2000, N=127; Isovalues for the stream function, the vorticity, the pressure and the kinetic energy

[7]. Of course the minimizing parameter becomes harder to compute as p increases. We list hereafter the optimal values of the parameters for $p = 1, 2, 3$

- $p = 1$ (Cauchy method)

$$\alpha_i^k = 1, \Delta t_k = \frac{< Ar^k, r^k >}{\|Ar^k\|^2}$$

- $p = 2$ (Enhanced Cauchy 1 (EC1) see [8, 9])
  We set

$$a = \|r^k\|^2,\ b =< Ar^k, r^k >,\ c = \|Ar^k\|^2, d =< A^2r^k, r^k >,\ e =< A^2r^k, Ar^k >, f =< A^2r^k, A^2r^k >,$$

$$\Delta t_k = \frac{fb - ed}{fc - e^2},\quad \alpha_1 = 1 - \frac{\Delta t_k e - d}{\Delta t_k^2 f},\ \alpha_2 = 1 - \alpha_1$$

- $p = 3$ (Enhanced Cauchy 2 (EC2))
  We set

$$a = \|Ar^k\|^2,\ b = \|A^2r^k\|^2,\ c = \|A^3r^k\|^2,\ d =< Ar^k, r^k >,\ e =< A^2r^k, r^k >,$$
$$f =< A^3r^k, r^k >,\ g =< A^2r^k, Ar^k >,\ hh =< A^3r^k, Ar^k >,\ ii =< A^3r^k, A^2r^k >$$

$$\Delta t_k = \frac{-hh\ ii\ e - g\ ii\ f + hh\ f\ b + d\ ii^2 - d\ c\ b + g\ c\ e}{(g^2\ c + hh^2\ b - a\ c\ b + a\ ii^2 - 2\ hh\ ii\ g)}$$

$$\alpha_1 = \frac{(ii\ f - ii\ \Delta t_k\ hh + (\Delta t_k)^2\ ii^2 - (\Delta t_k)^2\ b\ c - e\ c + \Delta t_k\ g\ c)}{((\Delta t_k)^2\ (-b\ c + ii^2))}$$

$$\alpha_2 = -\frac{(\Delta t_k\ ii\ f - hh\ (\Delta t_k)^2\ ii - dt\ e\ c + (\Delta t_k)^2\ g\ c - f\ b + \Delta t_k\ hh\ b + ii\ e - ii\ \Delta t_k\ g)}{((\Delta t_k)^3\ (-b\ c + ii^2))}$$
$$\alpha_3 = 1 - \alpha_1 - \alpha 2$$

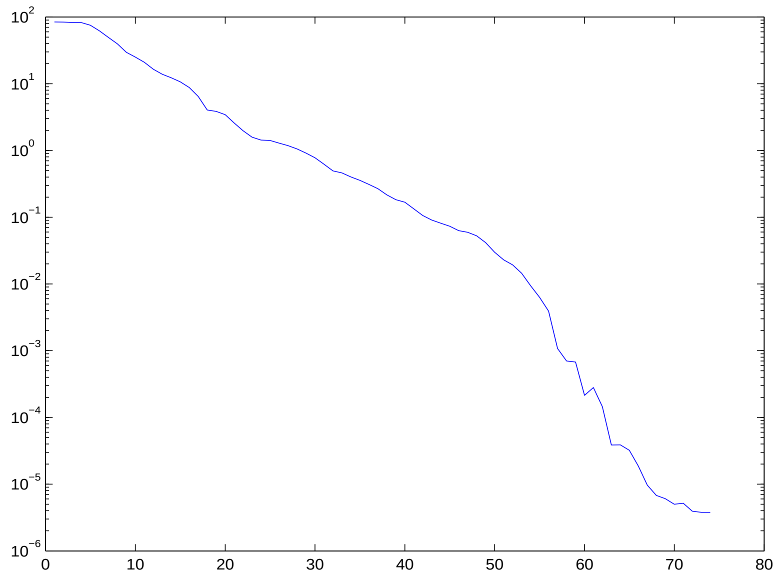

Figure 15: Steady NSE, Cavity B, Re=2000, N=127. Residual vs iterations